Progr Colloid Polym Sci (2004) 128: 232–238
DOI 10.1007/b97092

Paula S. Haddad
Evandro L. Duarte
Mauricio S. Baptista
Gerardo F. Goya
Carlos A.P. Leite
Rosangela Itri

Synthesis and characterization of silica-coated magnetic nanoparticles

Abstract The present work reports on the synthesis and properties of magnetic nanoparticles based on magnetite coated by a silica layer. A series of conditions was tested to allow the synthesis of the nanoparticles, usually performed in an aqueous medium, and could be efficiently coupled with the silica sol–gel process. The resulting particles were characterized by means of X-ray diffraction, transmission electron microscopy associated with electron energy loss spectra and electron spectroscopy imaging, Fourier transform IR, Mössbauer and magnetization measurements. Initially, magnetite particles with an average crystalline grain size of about 100 Å and a polydispersion of 30%, as revealed by X-ray diffraction and transmission electron microscopy analyses, respectively, were obtained with a mixture of $FeCl_2$ and $FeCl_3$ in aqueous and acid solution. The magnetization measurements, at room temperature, show that the particles are in the superparamagnetic regime. Magnetite was also synthesized in acid solutions in an alcoholic environment (25% methanol-to-base ratio), a medium that allows us to proceed with silica-coating by the sol–gel process in a one pot reaction. The resulting particles present size dispersion ranging from around 15 Å to about 200–300 Å as evidenced by electron micrographs. The superparamagnetic behavior is preserved, although its saturation magnetization value decreases from about 92 to about 50 emu g^{-1}, probably owing to the contribution of the smallest particles as well as to the surface spin disorder induced by addition of methanol to the synthesis medium. For higher values of the alcohol-to-base ratio, the resulting particles are amorphous, becoming crystalline under thermal treatment. When tetraethylorthosilicate is added to a solution containing 25% of methanol to base, iron oxides are SiO_2-coated at room temperature, as evidenced by electron spectroscopy imaging and Fourier transform IR spectroscopy. The magnetization results are dependent on the Si-to-Fe volume ratio, in such a way that the values decrease as the SiO_2 amount increases, reflecting the nanoparticle coating.

Keywords Magnetic nanoparticles · Sol–Gel synthesis · Silica coating · Superparamagnetism · Electron spectroscopy imaging

C.A.P. Leite
Instituto de Química, Universidade Estadual de Campinas, UNICAMP, CP 6154, 13083-970, Campinas, SP, Brazil

P.S. Haddad · M.S. Baptista
Departamento de Bioquímica, Instituto de Química, Universidade de São Paulo, Av. Lineu Prestes, 748, 05508-900 São Paulo, SP, Brazil

E.L. Duarte · G.F. Goya · R. Itri (✉)
Instituto de Física,
Universidade de São Paulo, CP 66318, 05315-970 São Paulo, SP, Brazil
e-mail: itri@if.usp.br
Tel.: +55-11-30917012

Introduction

Magnetic nanocomposites have been the subject of extensive investigation owing to their important properties and applications [1], such as information storage [2], color imaging [3], and magnetic refrigeration [4].

The preparation methods of ferrite-like nanocomposites (Fe_3O_4 or γ-Fe_2O_3) are very important owing to the fundamental and technological perspectives. Small particles exhibit very peculiar properties compared with those presented in bulk materials, and these peculiar properties can provide new ways of using magnetic structures also in biotechnology [5]. A challenging issue in the nanomagnetic field is to develop strategies to functionalize these particles. A new biocompatible magnetic nanoparticle covered by drugs would have potential application in medicine [6].

Several strategies are being tested to functionalize these particles, including reaction with dimercaptosuccinic acid [6], which has been used to graft a variety of molecules and biomolecules to magnetic nanoparticles [6–8]. However, this route usually provides relatively labile bridges with the magnetic nanoparticle [6–8]. Another possible route to graft these particles, which has received special attention in recent years, involves the use of an inorganic material such as silica [9–17]. This special interest arises from the fact that the silica grafting somehow stabilizes the particles in the ferromagnetic γ-Fe_2O_3 form, i.e., it decreases the transition efficiency to the antiferromagnetic α-Fe_2O_3 form with an increase in temperature [12, 15, 16]. It also provides a transparent layer that can be used to stabilize the particles in suspension, providing a route to easily further graft it with organic molecules [9, 10, 12, 18, 19].

There are basically two ways to obtain the γ-Fe_2O_3/SiO_2 composites:

1. Disperse the previously synthesized iron oxide particles in different sol–gel matrices. This is usually performed by coprecipitating the particles in aqueous solution, filtering and redispersing the precipitate in ethanol solution to perform the silica coating by silane hydrolysis and polymerization [9, 10, 11].
2. In situ precipitation of the magnetic nanoparticles during the matrix formation [12, 15–17], which does not involve the step of filtration and redispersion. However, this method can have relatively long gelation times, sometimes longer than 9 days [17, 20], and the solution has to be heated to relatively high temperatures (above 700 °C) [12, 16, 17, 20].

In the current work, an effort has been made to find an alternative route to prepare magnetic nanoparticles and to coat them with silica. Ferrite-like nanoparticles were prepared by mixing $FeCl_2$ and $FeCl_3$ acidic solutions (to avoid the formation of iron hydroxides) in an alcoholic environment and by adding tetraethylorthosilicate (TEOS) in an one-pot reaction scheme. With this procedure we would not need the filtration and redispersion step characteristic of method 1 nor the long gelation time and thermal treatment of method 2.

A variety of structural and spectroscopic methods were used to characterize these particles. Structural determination of nanoparticles was performed by means of X-ray diffraction (XRD). Fourier transform IR (FTIR) spectroscopy was used to identify the stretching vibration of Si–O–Fe. Transmission electron microscopy (TEM) with an energy filter was also carried out to observe the nanoparticle size and shape. Electron spectroscopy imaging (ESI) was used to probe the elemental distribution. Mössbauer and vibrating sample magnetometer (VSM) techniques, at room temperature, were used to characterize the magnetic properties of the nanoparticles.

Experimental

Materials

All reagents were obtained from commercial suppliers and were used without any further purification. Water was distilled in all-glass apparatus, filtered and deionized (Milli-Q water). All experiments were performed at room temperature of 23 ± 1 °C.

Synthesis

Three different kind of samples were studied. The first one was synthesized in an acidic medium according to the well-established protocol in the literature [21]. A 1.0-mL aliquot of $FeCl_2$ (Merck) (1.0 M) and 4.0 mL $FeCl_3$ (Merck) (0.5 M) prepared in 1.0 M HCl (Aldrich) were vigorously stirred, while 50.0 mL NH_3 (0.7 M) (Aldrich) was slowly dropped into the solution, resulting immediately in a black precipitate. At this stage, the precipitate was decanted, washed thoroughly with acetone and dried in vacuo. The second one involved the same iron mixture of acid solution in an alcoholic medium containing methanol (Merck) and base in a volume ratio of 25%. After the same washing and drying procedures as described for the fist sample, a black powder was also obtained. Both samples were crystalline at room temperature (see later). It is worthy of mention that solutions containing higher ratios of methanol to base were also investigated, but the nanoparticles obtained were amorphous at room temperature, becoming crystalline under thermal treatment at 500 °C for 2 h in a nitrogen atmosphere.

In order to obtain silica-coated magnetic nanoparticles at room temperature, TEOS was used as the Si source and was added to the 25% methanol-to-base solution just after the black precipitate had been formed. The amount of TEOS was changed depending on the desired Si-to-Fe volume ratio (10%, 20%, 30%, 50% and 70%). A brown gel was immediately obtained, and was washed with acetone. The nanoparticles were isolated by decantation.

Methods

XRD: Structural identification was performed by using a Rigaku-Denki powder diffractometer with a conventional X-ray generator (Cu Kα radiation $\lambda = 1.5418$ Å and a graphite monochromator)

coupled to a scintillation detector. The angular scanning performed on all samples ranged from 20° up to 70° with 0.05° step width. The average size of the nanoparticles was calculated from the full width at half maximum of the (311) reflection (spinel structure) using Scherrer's equation [22].

TEM: A Carl Zeiss CEM 902 transmission electron microscope equipped with a Castaing Henry–Ottensmeyer filter spectrometer within the column was used. One drop of the particle dispersion was deposited onto carbon-coated parlodion films supported in 300-mesh gold grids. The images were obtained using zero loss energy, low loss energies between 20 and 30 eV and specific elemental energies; they were recorded with a slow-scan CCD camera (Proscan) and processed in the AnalySis 3.0 system. Electron energy loss spectra in the range 70–150 and 680–760 eV for Si and Fe were acquired for use as a reference to ESI, in the CEM-902 transmission electron microscope, by using the parallel acquisition method [23].

FTIR: The IR spectra were recorded using a Nicolet IMPACT 400 spectrophotometer in a wavenumber range from 4,000 to 400 cm^{-1}, at a resolution of 2 cm^{-1}, using KBr pellets.

VSM: A VSM was used to obtain the magnetization versus magnetic field loop (M versus H) at room temperature up to H = 20 kOe. The apparatus was calibrated with a Ni pattern. The magnetization measurements were carried out on a known quantity of sample powder, slightly pressed and conditioned in cylindrical holders of Lucite.

Mössbauer: The measurements were performed with a conventional constant-acceleration spectrometer in a transmission geometry with a source of about 50 mCi ^{57}Co in a Rh matrix between 78 and 296 K. Hyperfine parameters, such as the distribution of the hyperfine magnetic field (B), the isomer shift (IS) and the quadrupole shift (QS), were determined by the NORMOS program.

Results and discussion

Structural and morphological evaluations

X-ray diffraction data, typical of a spinel structure [24], obtained from samples prepared in acid solution in the absence (sample 1) and in the presence of an alcoholic medium (no TEOS, sample 2) are shown in Fig. 1. In fact, such a structure corresponds to magnetite, as demonstrated by the Mössbauer data presented later. The analysis of the main X-ray reflection (311) peak width and position by using the Debye–Scherrer equation led to a mean grain size of 100 Å for sample 1 and 170 Å for sample 2 (without TEOS). Then, the presence of methanol in the synthesis environment seems to induce the formation of larger magnetic particles.

At the same time, the TEM micrograph (Fig. 2a) reveals that sample 1 is constituted by particles with well-defined spherical shape contours with a mean dimension of 60 Å and a polydispersity of about 30%; therefore, the X-ray reflection width is predominantly weighted by the largest particles. However, lower-quality micrographs were obtained from sample 2 synthesized in an alcoholic medium. Firstly, most of the images did not contain isolated particles, making it difficult to define their morphology and size. Secondly, the images show

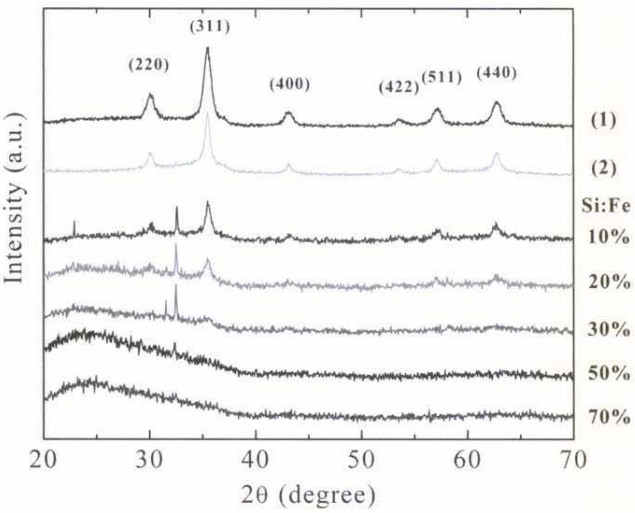

Fig. 1 X-ray powder diffraction from samples synthesized in an acidic medium (*1*), and in a methanolic medium (25% methanol-to-base ratio) with increasing Si-to-Fe volume ratio, as indicated in the figure, ranging from 0% (*2*) to 70%, at room temperature

particles with a very broad size distribution, including small particles of average sizes of 15 Å (Fig. 2b) and large particles with dimensions of about 200–300 Å (Fig. 2c). Therefore, the presence of methanol in the synthesis medium also seems to amplify the polydispersity of the system.

It should be remarked that the magnetic nanoparticles prepared by the usual coprecipitation method in aqueous solution [25] have the same features, revealed by XRD and TEM, as those obtained in acidic solution (sample 1).

For samples containing a Si-to-Fe volume ratio of 10% and 20% the main X-ray reflections (Fig. 1) still indicate the spinel-like crystalline structure and the nanoparticles keep their average grain size of about 170 Å. The extra peak at $2\theta \tilde{} 32.5°$ is identified as the SiO_2 reflection, evidencing its formation during the synthesis. Further, a large band is observed in the angular range from 20° to 40° that increases with addition of silica to the system. This behavior indicates the formation of an amorphous silica phase, in such a way that for large silica content (30, 50 and 70% of Si to Fe) there is a predominance of the amorphous phase attributed to amorphous SiO_2 in the X-ray spectra. It should be emphasized, however, that dark-field electron micrographs (data not shown) revealed the preservation of some crystalline phase.

The FTIR spectra obtained from samples containing 10–70% of Si to Fe are shown in Fig. 3. The frequencies of the most important bands are depicted in Fig. 3. FTIR spectroscopy is a helpful technique to identify the stretching vibrations of Si–O, Si–O–Fe and Fe–O–Fe bonds [26–30]. The FTIR spectra of all the samples

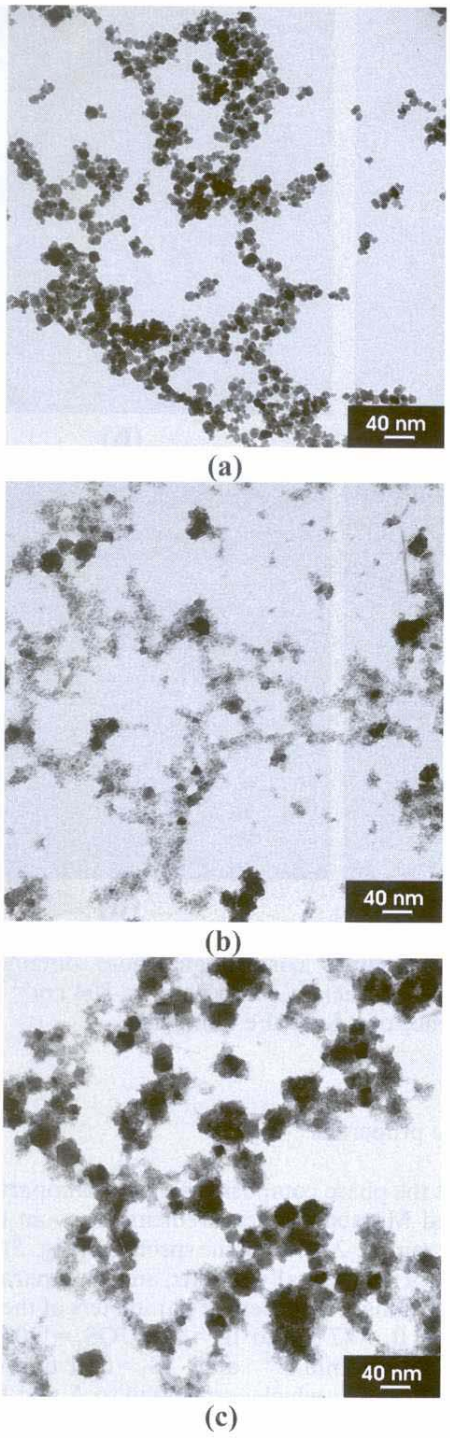

Fig. 2 Transmission electron microscopy micrographs recorded from samples prepared in **a** an acidic environment (sample 1), and a methanolic environment (25% methanol-to-base ratio) (sample 2) representing **b** smaller nanoparticles and **c** larger ones

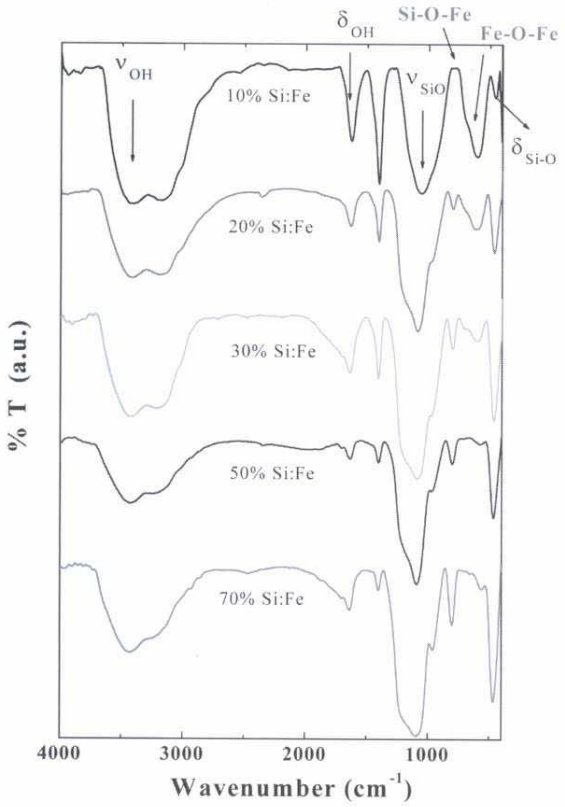

Fig. 3 Fourier transform IR spectra from nanoparticles synthesized in a methanolic medium (25% methanol-to-base ratio) with increasing Si-to-Fe volume ratio from 10% to 70%, at room temperature

(Fig. 3) show bands at 3,440 and 1,640 cm^{-1}, assigned to ν_{OH} and δ_{OH}, respectively. The bands around 1,100, 1,400 and 470 cm^{-1} are attributed to the Si–O bond. The δSi–O increases as the amount of silica increases. The sharp band around 800 cm^{-1} suggests the presence of Si–O–Fe bonds. The bands at 600 cm^{-1} must be evidence of a Fe–O–Fe bond [31–33]. The increase in the silica content implies the decrease of such a band, whereas the Si–O–Fe band increases. The bands are not shifted significantly; therefore, the FTIR analysis suggests the binding of silica to the iron oxide nanoparticles at the surface.

In order to certify that these samples were actually silica-coated, we made use of the electron energy loss spectra and ESI of the particle surface. The Si and Fe elemental maps for 10% and 50% of Si-to-Fe samples are shown in Fig. 4. As one can see, Fig. 4a evidences (for the sample prepared with 10% of Si to Fe) the elemental Si map (i.e., the bright region corresponds to high elemental Si concentration), whereas Fig. 4b represents the elemental Fe distribution for the same sample. Considering that the particles are coated by silica, one can interpret the ESI results by comparing both images. Note that in the same region of the elemental Si map (clear region in Fig. 4a) there is an underlying Fe

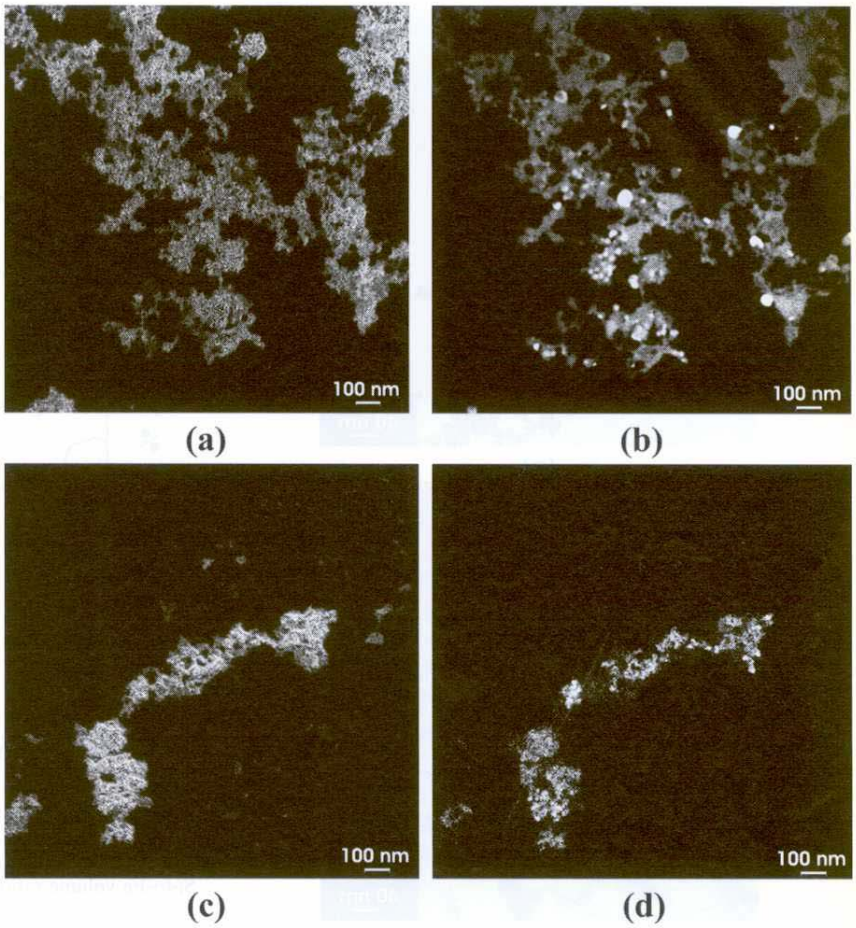

Fig. 4 Electron spectroscopy imaging micrographs of **a** Si and **b** elemental Fe maps from a sample with a Si-to-Fe ratio of 10% and **c** Si and **d** elemental Fe maps from a sample with a Si-to-Fe ratio of 50% (see text for details)

component (bright region in Fig. 4b). This suggests the superposition of a silica layer over iron oxide particles. Similar behavior is observed for 50% of Si to Fe (Fig. 4c, d). These findings corroborate those obtained from FTIR results, where a sharp band at 804 cm^{-1} suggests the presence of a Si–O–Fe bond [12].

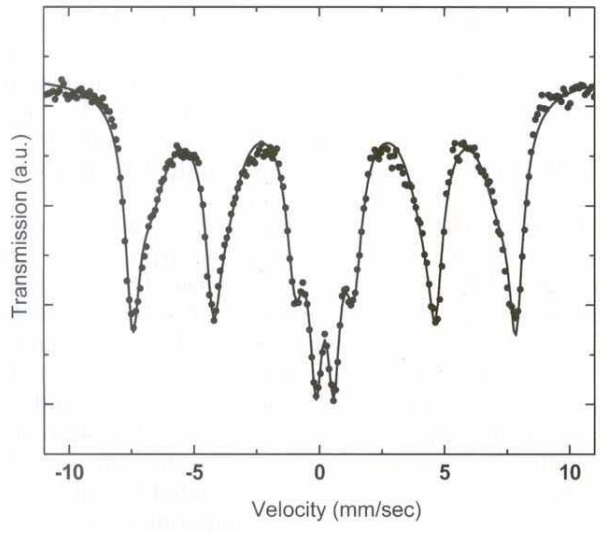

Fig. 5 Mössbauer spectra (*circles*) of the magnetite sample 2 at room temperature. The *solid line* is the best fit to the experimental data

Magnetic properties

To assess the phase composition of the nanoparticles, we performed Mössbauer measurements at room temperature. For sample 2 (0% Si), the spectrum (Fig. 5) displays a mixture of magnetically blocked and superparamagnetic contributions. The hyperfine parameters of the blocked sextets are $B_1 = 47$ T and $B_2 = 43$ T, $QS_1 = 0.00$ mm s^{-1} and $QS_2 = 0.00$ mm s^{-1} and $IS_1 = 0.31$ mm s^{-1} and $IS_2 = 0.33$ mm s^{-1}, which correspond to A and B sites of the magnetite phase [34–36]. For samples with higher silica contents, the spectra showed only a superparamagnetic doublet, and thus no information about the phase can be extracted. Low-temperature spectra (80 K) were obtained, but the superparamagnetic state still persists at this temperature; therefore, data at 4.2 K are being currently obtained to identify the magnetic phase in the blocked state.

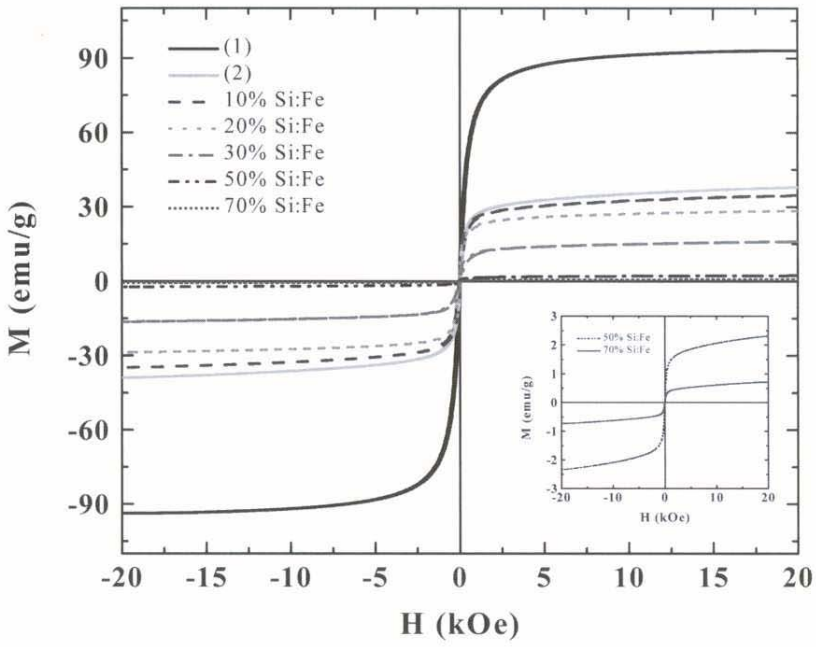

Fig. 6 Magnetization hysteresis curves at room temperature from samples prepared in: an acid medium (*1*), and in a methanolic medium (25% methanol-to-base ratio) with increasing Si-to-Fe volume ratio, as indicated in the figure, ranging from 0% (*2*) to 70%, at room temperature. The *inset* amplifies the magnetic behavior from samples containing the highest amount of silica

Typical magnetization curves obtained by VSM analysis are shown in Fig. 6. The samples are found to be superparamagnetic from the complete reversibility of the M–H curve recorded at room temperature [34]. The saturation magnetization (M_s) of sample 1 prepared in an acid medium (also in water, data not shown) was $M_s = 92(2)$ emu g^{-1}, which is coincident with the value for bulk magnetite [37], reinforcing the Mössbauer results. On the other hand, the strong decrease of M_s (about 38 emu g^{-1}) observed on addition of methanol (sample 2) may be due to the increase in the particle size polydispersity, as evidenced by XRD (Fig. 1) and TEM images (Fig. 2). The smaller particles usually yield surface spin disorder and thus lower magnetization values [35, 38]. With addition of TEOS to the system, M_S decreases until about 1 emu g^{-1} for a 70% Si-to-Fe volume ratio (Fig. 5). This behavior is, indeed, expected once a nonmagnetic material such as SiO was added to this system $_2$ [33].

Conclusions

We have presented an alternative method to synthesize silica-coated magnetic nanoparticles, by mixing $FeCl_2$ and $FeCl_3$ acid solutions in an alcoholic medium, followed by a sol–gel process using TEOS as the Si source, that produced a gel phase, immediately. ESI and FTIR measurements give strong support to the conclusion that the iron oxide particles are silica-coated. Moreover, Mössbauer data and XRD reflections are consistent with the magnetite structure for nanoparticles prepared in a solution containing Si-to-Fe volume ratios of 10% and 20%. The particles have a mean crystalline grain size of about 170 Å, in agreement with that obtained in the absence of TEOS. The magnetic properties of these particles are preserved, in such a way that superparamagnetic behavior is still observed, although their saturation magnetization values decrease slightly, probably owing to an increase of the surface spin disorder and nonmagnetic SiO_2 coating. Therefore, we are now able to proceed towards the synthesis of a new magnetic particle that contains photoactive molecules attached to its surface, by functionalizing the silica layer with photoactive molecules [18].

Acknowledgements The authors thank CNPq, CAPES/PROCAD, FAPESP and Millenium Institute/IQ-UNICAMP.

References

1. Beecroft LL, Ober CK (1997) Chem Mater 9:1302
2. Awschalom DD, DiVicenzo DP (1995) Phys Today 43
3. Ziolo RF, Giannelis EP, Weinstein BA, O' Horo MP, Ganguly BN, Mehrotra V, Russel MW, Huffman DR (1992) Science 257:219
4. McMicheal RD, Shull RD, Swartzendruber LJ, Bennett LH, Watson RE (1992) J Magn Mater 11:29
5. Häfeli U, Schüt W, Teller J, Zborowski M, (1997) Scientific and clinical applications of magnetic carriers, 1st edn. Plenum, New York
6. Roger J, Pons JN, Massart R, Halbreich A, Braci JC (1999) Eur Phys J A 5:321
7. Fauconnier N, Pons JN, Roger J, Bee A (1997) J Colloid Interface Sci 194:427
8. Safarik I, Safarikova M (1999) J Chromatogr B 722:33
9. Klotz M, Ayral A, Guizard C, Ménaer C, Cabuil V (1999) J Colloid Interface Sci 220:357
10. Ma M, Zhang Y, Yu W, Shenm HY, Zhang HQ, Gu N (2003) Colloids Surf A 212:219
11. Morales MP, Munoz-Aguado MJ, Garcia-Palacio JL, Lazaro FJ, Serna CJ (1998) J Magn Magn Mater 183:232
12. Moreno EM, Zayat M, Morales MP, Serna CJ, Roig A, Levy D (2002) Langmuir 18:4972
13. Tartaj P, González-Carreño T, Sena CJ (2003) J Phys Chem 107:20
14. Del Barco E, Asenjo J, Zhang XX, Pieczynsky R, Juliá A, Tejada J, Ziolo RF, Fiorani D, Testa AM (2001) Chem Mater 13:219
15. Cannas C, Casula MF, Concas G, Corrias A, Gatteschi D, Falqui A, Musinu A, Sangregorio C, Spano G (2001) J Mater Chem 1:3180
16. Cannas C, Gatteschi D, Musinu A, Piccaluga G, Sangregorio C (1998) J Phys Chem B 102:7721
17. Ennas G, Musinu A, Piccaluga G, Zedda D, Gatteschi D, Sangregorio C, Stanger JL, Concas G, Spano G (1998) Chem Mater 10:495
18. Rodrigues MA, Tada DB, Politi MJ, Baptista MS (2002) J Non-Cryst Solids 304:116
19. Rodrigues MA, Politi MJ, Miranda MTM, Bemquerer MP, Brochsztain S, Baptista MS (2002) Chem Lett 6:604
20. Savii C, Popovici M, Enache C, Subrt J, Niznansky D, Bakardzieva S, Caizer C, Hrianca I (2002) Solid State Ionics 151:219
21. Berger P, Adelman NB, Beckamn KJ, Campbell DJ, Ellis AB, Lisensky GC (1999) J Chem Educ 76:943
22. Klug HP, Alexander LE (1974) X-ray diffraction procedures for polycrystalline and amorphous materials, 2nd edn. Wiley-Interscience, New York
23. Costa CAR, Leite CAP, Galembeck F (2003) J Phys Chem B 107:4747
24. Itri R, Depeyrot J, Tourinho FA, Sousa MH (2001) Eur Phys J E 4:201
25. Massart R (1983) IEEE Trans Magn 17:1247
26. Nogami M, Asuha N (1993) J Mater Sci Lett 12:1705
27. Chaneac C, Tronc E, Jolivet JP (1996) J Mater Chem 6:1905
28. Ying JY, Benziger JB, Navrostsky A (1993) J Am Ceram Soc 76:2571
30. Ayers MR, Song XY, Hunt AJ () J Mater Sci 31:6251
31. Nyquist RA, Kagel RO (1971) Infrared spectra of inorganic compounds: 3,800–45 cm^{-1}, 1st edn. Academic, New York
32. McDevitt NT, Baun WL (1964) Spectrochim Acta 20:799
33. Del Monte F, Morales MP, Levy D, Fernandez A, Ocaña M, Mollins E, ÓGray K, Serna CJ (1997) Langmuir 13:3627
34. (a) Biddlecombe GB, Gun'ko YK, Kelly JM, Pillai SC, Coey JMD, Venkatesan M, Douvalis AP (2001) J Mater Chem 11:2937; (b) Rajendran M, Pullar RC, Bhattacharya AK, Das D, Chintalapudi SN, Majumdar CK (2001) J Magn Magn Mater 232:71
35. Goya GF, Berquó TS, Fonseca FC, Morales MP (2003) J Appl Phys 94:3520
36. Voogt FC, Hibma T, Smulders P, Niesen L (1997) J Cryst Growth 174:440
37. Cullity BD (1972) Introduction to magnetic material, 1st edn. Addison-Wesley, London
38. Dormann L, Fiorani D, Tronc E (1997) In: Prigogine I, Rice SA (eds) Advances in chemical physics. New York